Nucleus Isthmi, Pars Semilunaris as a Key Component of the Tectofugal Visual System in Pigeons

BURKHARD HELLMANN,[1]* MARTINA MANNS,[2] AND ONUR GÜNTÜRKÜN[1]
[1]Biopsychologie, Fakultät für Psychologie, Ruhr-Universität-Bochum,
44780 Bochum, Germany
[2]Molekulare Neurobiochemie, Fakultät für Chemie, Ruhr-Universität-Bochum,
44780 Bochum, Germany

ABSTRACT

The avian isthmic nuclei are constituted by a group of structures reciprocally connected with the tectum opticum and considered to play a role in the modulation of intratectal processes. Although the two larger isthmic nuclei, the n. isthmi pars parvocellularis (Ipc) and the n. isthmi pars magnocellularis (Imc), have been studied in detail previously, the third and smallest of this group, the n. isthmi pars semilunaris (SLu), has been largely neglected. The present study demonstrates this isthmic component to be characterized by a unique connectivity and immunohistochemical pattern: 1) SLu receives tectal afferents and projects back onto the outer retinorecipient tectal layers; 2) it projects bilaterally onto the nucleus rotundus and thus modulates the ascending tectofugal system; 3) in addition, previous studies have demonstrated SLu projections onto the lateral spiriform nucleus (SpL), which mediates basal ganglia output onto the tectum. In that SpL projects onto the deep layers of the tectum, SLu indirectly modulates descending tectal output patterns. Taken together, the role of SLu goes far beyond a local modulation of intratectal processes. Instead, this isthmic structure is likely to play a key role in the topographically organized modulation of the ascending and, at least indirectly, also the descending projections of the optic tectum. J. Comp. Neurol. 436:153–166, 2001. © 2001 Wiley-Liss, Inc.

Indexing terms: isthmic nuclei; tectum opticum; nucleus rotundus; extrageniculocortical pathway; visuomotor integration; birds

The nucleus isthmi is a visual midbrain structure with topographically organized and reciprocal connections to the midbrain roof. By this definition, it is present in most vertebrates, including fish (Sakamoto et al., 1981; Northcutt, 1982), amphibians (Gruberg and Udin, 1978), reptiles (Wang et al., 1983; Welker et al., 1983; Künzle and Schnyder, 1984), birds (Hunt et al., 1977), and mammals (Graybiel, 1978; Baleydier and Magnin, 1979; Sherk, 1979; Künzle and Schnyder, 1984). This widespread distribution points to a critical role in tectally based visual information processing (Bagnoli et al., 1979; Sereno and Ulinski, 1987; Wang and Frost, 1991; Wiggers and Roth, 1991). In comparison to other classes of vertebrates, birds possess a highly differentiated tectofugal visual system. In pigeons, about 90% of the retinal ganglion cells project onto the tectum, from which multiple parallel projection streams ascend to different regional domains of the diencephalic nucleus rotundus (Hellmann and Güntürkün, 2001), which itself is characterized by a spatial subdiffer-

entiation of function (Wang et al., 1993). A high degree of complexity is also apparent in the isthmus, which exhibits a threefold subdifferentiation. This morphological segregation suggests a spatial separation of function and opens the possibility of studying different modulatory actions of the isthmus independently (Wang et al., 1995).

In pigeons, the nucleus isthmi can be subdivided into the nucleus isthmi pars parvocellularis (Ipc), pars magnocellularis (Imc), and pars semilunaris (SLu), all of them receiving ipsilateral tectal input in parallel (Hunt and Künzle, 1976). Apart from this general correspondence,

Ipc and Imc differ with respect to their tectal connectivity pattern, their neurotransmitter expression, and their functional properties: Ipc receives strong and topographically ordered input from tectal layer 10 neurons and constitutes an inhibitory return projection onto the outer retinorecipient layers 2–5 (Hunt and Künzle, 1976; Wang et al., 1995; Woodson et al., 1991). In contrast, Imc receives only sparse and probably nontopographically arranged tectal input (Hunt and Künzle, 1976), whereas its output ramifies within deep tectal layers 12–14 (Hunt and Brecha, 1984; Wang and Wang, 1990), where it exerts excitatory influences on tectal units (Wang et al., 1995). With the exception of some GABAergic cells within its rostral pool (Hunt et al., 1977; Wang et al., 1993), most Ipc neurons are cholinergic (Bagnoli et al., 1992; Medina and Reiner, 1994; Sorenson et al., 1989), whereas virtually all Imc neurons express γ-aminobutyric acid (GABA; Domenici et al., 1988; Granda and Crossland, 1989; Tömböl and Németh, 1998; Veenman and Reiner, 1994).

SLu is the smallest of the three isthmic nuclei in birds. This double-layered cell group is located ventromedially adjacent to the Ipc in the mesencephalic tegmentum (Güntürkün, 1987). Like the Ipc, SLu exhibits tight reciprocal connections with the tectum (Hunt and Künzle, 1976), and its neurons are also cholinergic (Medina and Reiner, 1994). Because these hodological and biochemical similarities indicated a close functional similarity between Ipc and SLu, physiological examinations have neglected the Slu. However, SLu is the only isthmic structure that establishes extratectal connections, with projections onto the lateral spiriform nucleus (SpL), which transfers basal ganglia output to the tectum (Reiner et al., 1982a,b). The present immunohistochemical and tract-tracing work shows, in addition, that the connectivity pattern of the SLu goes far beyond what has conceived until now and makes it likely that this neglected isthmic structure is a key component of the tectofugal system.

MATERIALS AND METHODS

Forty-four adult pigeons (*Columba livia*) of unknown sex and from local breeding stocks were used. Immunohistochemistry was performed in six animals to reveal the distribution of antigens against GABA, cholineacetyltransferase (ChAT), and ionotrophic glutamate receptor subunits. Thirty-six animals received injections of different tracers into the optic tectum, the nucleus rotundus, or the lateral spiriform nucleus. For anterograde pathway tracing, biotinylated dextran amine (BDA; 10,000 MW; lysine-fixable, 10% in 2% DMSO; Molecular Probes, Leiden, The Netherlands) was used. Retrograde pathway tracing was performed with the fluorescing tracers Texas red dextran amine (TDA) and fluorescein dextran amine (FDA; both 10,000 MW; lysine-fixable, 8% in 2% DMSO; Molecular Probes). In addition, choleratoxin subunit B (CtB; 1% in A.dest.; Sigma, Deisenhofen, Germany) was used. All experiments were carried out according to the specifications of the German law for the prevention of cruelty to animals.

Tracing experiments

Prior to surgery, the pigeons were anesthetized with equithesin (0.33 ml/100 g body weight) and were placed into a stereotaxic apparatus (Karten and Hodos, 1967). For tectal tracer injections, a modified device was used

TABLE 1. Antibodies Used and Their Concentrations

Antigen	Primary antibody	Secondary antibody
CtB	Goat anti-CtB, 1/20,000; Sigma	Biot. rabbit anti-goat, 1/200; Vector
	Goat anti-CtB, 1/8,000; Sigma	Fluorescein rabbit anti-goat, 1/75; Vector
GABA	Rabbit anti-GABA, 1/10,000; Sigma	Biot. goat anti-rabbit, 1/200; Vector
Glu R1	Rabbit anti-GluR1, 1/500, Chemicon	Biot. goat anti rabbit, 1/200; Vector
Glu R2/3	Rabbit anti-GluR2/3, 1/500; Chemicon	Biot. goat anti-rabbit, 1/200; Vector
ChAT	Goat anti-ChAT, 1/1,000; Chemicon	Biot. rabbit anti-goat, 1/200; Vector

that allowed lateral rotation of the head along the longitudinal axis over 100° to the left and to the right. The scalps were infiltrated with Xylocaine and subsequently incised either between eye and auditory meatus (tectal injections) or dorsally along the midline of the head (rotundal injections). Next, the scull was opened with a dental drill and a glass micropipette (outer tip diameter 20–25 μm) mounted to a mechanic pressure device (WPI Nanoliterinjector) was inserted into the rotundus or optic tectum according to stereotaxic coordinates of the pigeon brain atlas by Karten and Hodos (1967). The different tracers were injected in steps of 2 nl over a period of 20–30 minutes. Overall injection volume ranged between 30 nl (CtB) and 70 nl (dextran amines). Subsequently, the pipette was removed and the skin was infiltrated again with Xylocaine and sutured.

After survival times ranging from 2 days (rotundal and tectal CtB applications) to 8 days (rotundal dextran amine injections), the animals received an injection of 200 units sodium heparin and were then deeply anesthetized with an overdose of equithesin (0.55 ml/100 g body weight). The pigeons were perfused through the heart with 100 ml 0.9% (w/v) sodium chloride and 800 ml ice-cold 4% paraformaldehyde in 0.12 M phosphate buffer (PB), pH 7.4. The brains were removed and stored for 4 hours in fixative with a supplement of 15% sucrose (w/v). Subsequently, the brains were stored overnight in a solution of 30% sucrose in 0.12 M PB. On the following day, the brains were cut in frontal plane at 35 μm on a freezing microtome, and the slices were collected in PB containing 0.1% sodium azide (w/v).

Immunohistochemistry

For immunohistochemical demonstration of various antigens, pigeons were perfused as described for the tracing experiments, with the exception that primary and secondary fixatives additionally contained 0.2% glutaraldehyde. Immunhistochemical visualization was performed either according to the immuno-ABC-DAB or the immunofluorescence technique.

Sections were reacted freely floating. Only in case of the immuno-ABC-DAB technique were sections placed first for 35 minutes in 1% hydrogenperoxidase/50% ethanol to reduce endogenous peroxidase activity. After washing, sections were incubated for 36 hours at 4°C in the primary antibody solution [in 0.12 M PB after the addition of 2% NaCl (w/v), 0.3% Triton X-100 + 0.1% sodium-azide (w/v), and 5% normal serum from the host of the secondary antibody; see Table 1]. After being rinsed, the sections were incubated for 60 minutes at room temperature in the

biotinylated secondary antibody (in 0.12 M PB + 2% NaCl + 0.3% Triton X-100; see Table 1).

Brain slices containing either BDA or the secondary biotinylated antibody were additionally reacted freely floating according to the avidin-biotin-peroxidase technique (ABC). After rinsing, sections were incubated for 60 minutes in ABC solution (Vectastain ABC-Elite Kit; Vector, Wiesbaden, Germany; 1/100 in 0.12 M PB + 2% NaCl + 0.3% Triton X-100). After additional washing, the peroxidase activity was detected using a heavy metal-intensified 3'3-diaminobenzidine (DAB; Sigma, Deisenhofen, Germany) reaction (Adams, 1981), modified by the use of β-d-glucose/glucose-oxidase (Sigma) instead of hydrogenperoxidase (Shu et al., 1988). The sections were mounted on gelatin-coated slides, dehydrated, and coverslipped with Permount (Fisher Scientific, Fair Lawn, NJ). Some sections were counterstained with cresyl violet.

Sections from animals that had received fluorescent tracer injections or that were used with a secondary fluorescent antibody were mounted on gelatin-coated slides, air dried, and coverslipped with ProLong Antifade Kit (Molecular Probes). Sections were viewed with an Olympus BH2 epifluorescence microscope with the following filter settings: FDA, Olympus IB-set with additional shortpass emission filter G520; TDA, Chroma filters (Brattleboro, VT) with excitation filter HQ-577/10, dichroic mirror Q-585LP, and emission filter HQ-645/75.

Evaluation

Tracer injection sites were reconstructed using an Olympus BH2 microscope. Structures were drawn using PC software Designer 3.1 (Micrografx). For this, a digitized picture of the section was displayed on a computer monitor, using a black-and-white video camera (Kappa CF 8; Gleichen, Germany) attached to the microscope and a PC-based computer hardware configuration (Soft Imaging System, Münster, Germany). Intrarotundal tracer diffusion area was measured with the image-analyzing software SIS Analysis 3.0 (Soft Imaging System). The amount of double-labeled cells in fluorescing sections was determined with a 40× objective for three different focus planes by manually marking fluorescein-labeled cells in digital images and by a projection of these marks onto the corresponding digital image with Texas red labeling. Photographic documentation was carried out with a 35 mm camera system attached to the microscope using Agfa APX 25, Agfa APX 100, or Kodak Ectachrome 200 film. Digital images of double-labeled SLu cells resulting from tectal and rotundal tracer injections were recorded with a confocal laser scanning microscope (Zeiss LSM 510 attached to a Zeiss Axiovert 100M). Color images were processed with Photoshop 5.5 software (Adobe, Mountain View, CA). Color balance, contrast, and brightness were adjusted to a variable extent to meet satisfying output results with the Fuji "MediaLab" printer device.

RESULTS

The nucleus semilunaris is located at the lateral border of the mesencephalon, just between the tectal hemisphere and the lateral tegmentum. Dorsolaterally it adjoins the Ipc at rostrocaudal levels A1.7 to A2.2. In Nissl-stained material, SLu somata are seen to be ovoid, with mean diameters of 7/15 μm (short/long axes). Most of these perikarya cluster at the lateral margin, where they form two dorsoventrally oriented rows within the ventral SLu (Fig. 1). Cell density was medially 1.45 times higher than laterally. Somata within the dorsal SLu were circularly arranged with their long axes often oriented radially. Gallyas myelin staining revealed the SLu to be surrounded by dense fiber bundles (Fig. 2).

Tectal tracer injections

In general, the results demonstrated the existence of reciprocal connections between tectum opticum and SLu. CtB as well as fluorescent dextran injections into the tectum resulted in a retrograde labeling of numerous ipsilateral SLu somata, which were intermingled with diffuse anterograde fiber fillings. As in Nissl-stained material, the majority of retrogradely labeled somata were located at the outer margin of the SLu. The dendritic processes of these multipolar cells extended primarily radially into the central, cell-poor regions, where dendritic processes of the lateral and medial cell rows intermingled. Tectal BDA injections resulted in little somatic but often in a dense anterograde fiber labeling within the ipsilateral SLu. Axons entered SLu rostrolaterally and ramified several times to constitute a network of very fine irregularly oriented processes with highest densities in the central, cell-poor regions.

Focal tectal tracer applications revealed a tight topographic arrangement of reciprocal tectoisthmic connections. The rostrodorsal and the ventrocaudal tectum received input from and projected onto the rostrodorsal and the ventrocaudal SLu, respectively. As compared to sole anterograde labeling in correspondingly injected BDA cases, tectal CtB injections revealed a nearly exact overlap of anterogradely labeled fine fiber processes and retrogradely labeled somata within SLu (Fig. 3a). This arrangement points to strict reciprocity in the tectoisthmic connectivity. Double injections of different fluorescent dextran amines into the dorsal as well as the ventral tectum revealed a complete spatial segregation of retrogradely labeled SLu efferents; double-labeled neurons were not observed (Fig. 4a).

Although CtB injected cases generally revealed retrogadely labeled cells within all isthmic nuclei, only a subset of BDA cases with substantial tracer spread in the outer retinorecipient tectal layers 2–7 (n = 4) exhibited retrograde BDA filling of SLu somata. The remaining cases with BDA spread restricted nearly completely to the intermediate and deeper tectal layers 8–14 revealed an anterograde fiber, but a very poor retrograde somata labeling within the SLu. Beneath the isthmic projection, the tectal double injections of fluorescent dextrans demonstrated a topographically ordered input to the tectum from the pretectal nucleus spiriformis lateralis (SpL); dorsal or ventral tectal tracer injections resulted in the retrograde labeling of somata clustering predominately within the dorsal or ventral SpL, respectively (Fig. 4b).

Rotundal tracer injections

Our data demonstrate a substantial projection of the SLu onto the entire ipsilateral nucleus rotundus. Rotundal CtB injections (n = 20) always resulted in retrograde labeling of several neurons within the ipsilateral SLu. Intrarotundal CtB spread ranged between 11% and 51% of the entire rotundal area in frontal sections. Counts of CtB-labeled somata in every fifth section of the SLu revealed between 64 and 392 retrogradely labeled cells.
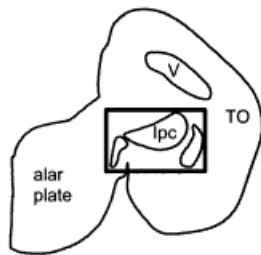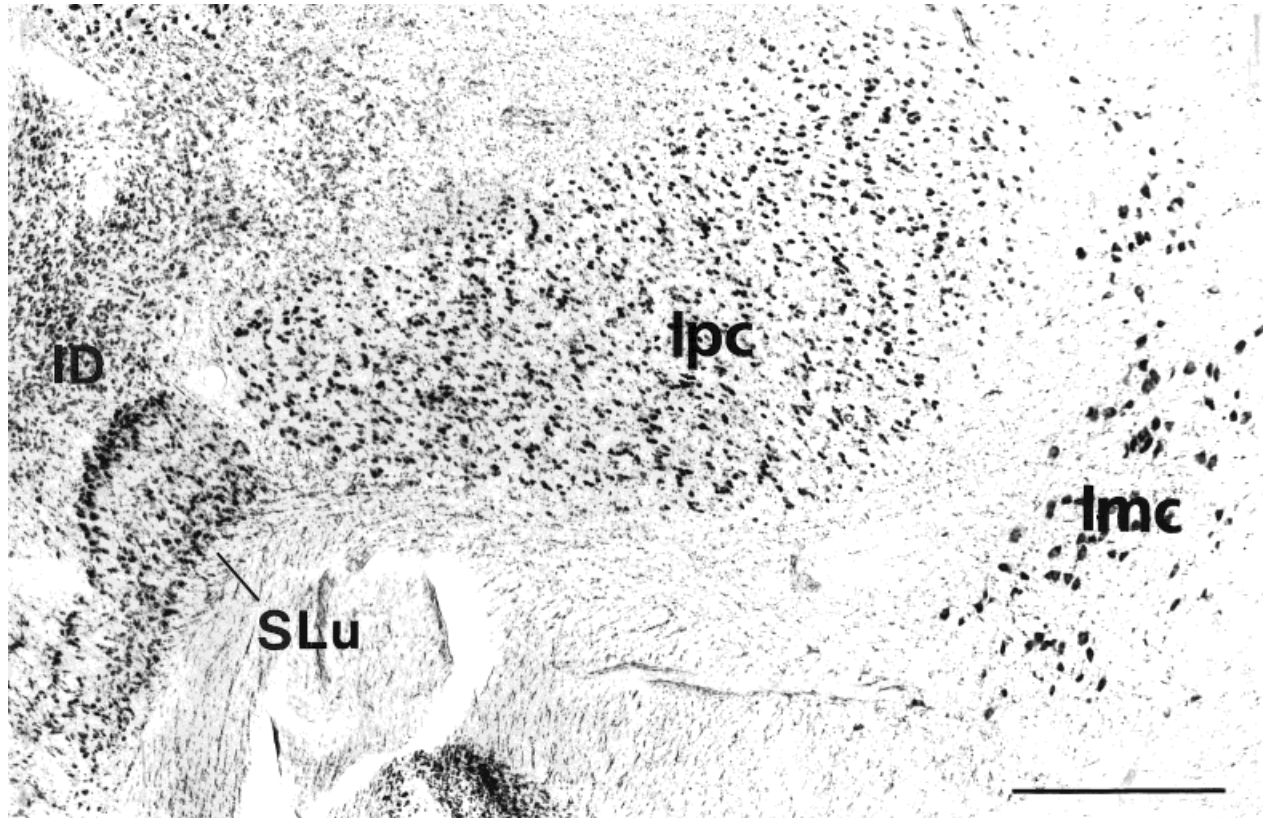
Fig. 1. Section of the caudal midbrain with the cresyl violet-stained isthmic cell groups n. isthmi pars magnocellularis (Imc), pars parvocellularis (Ipc), and pars semilunaris (SLu). In addition, the location of the disseminated nucleus, which is presumed to be a further isthmic component (ID; Medina and Reiner, 1994) is indicated. Within the SLu, cells are not distributed homogeneously but cluster at its medial and lateral margins. Scale bar = 500 μm.

These neurons had multipolar ovoid somata and were located primarily at the outer margins of the Slu, with their dendritic processes ramifying predominantly within the central core (Fig. 6a–c). Thus, they exhibited the same morphological features as retrogradely labeled cells after tectal CtB injections.

Focal CtB injections revealed a topography of semilunar projections onto nucleus rotundus: Caudal rotundal injections [n = 3; A5.2–A5.65 according to the pigeon brain atlas (Karten and Hodos, 1967)] labeled 72% (SD 16.3) of cells [mean number 138 (SD 42.8) counted in one fifth of all sections] within the dorsal SLu (Fig. 6a), whereas all other rotundal injections as well as those located within n. triangularis (n = 14) caused retrograde somatic labeling primarily throughout the remaining SLu, with 74% (SD 7.6) of cells [mean number 186 (SD 46.0) counted in one-fifth of all sections] located in the central and ventral portion (Fig. 6b,c). Only within the rostralmost tip of the SLu, neuronal somata were labeled without obvious spatial segregation after all rotundal injections.

Combined multiple tectal TDA applications and focal rotundal CtB (n = 3), with the latter tracer visualized via fluorescein-coupled secondary antibodies, revealed double-labeled somata within SLu (Fig. 5). About 46% (SD 16.2) of fluorescein-labeled rotundally projecting SLu somata also contained the tectally applied tracer.

In that retrogradely labeled SLu somata could in principle also result from extrarotundal tracer spread at the cannula track, additional CtB injections into the dorsal thalamus (n = 3) as well as into the nucleus lentiformis mesencephali and the ventrolateral component of nucleus principalis precommisuralis (n = 2) were performed. They revealed no labeled cells within SLu. In addition, it should be noted that rotundal BDA injections (n = 5) never resulted in anterograde labeling of fibers within the SLu.

Contralateral projections of the nucleus semilunaris

Rotundal CtB injections also revealed some retrogradely labeled neurons within the margin of the contralateral SLu. In two animals, two and three cells (counted in one-tenth of all sections) were located directly within the dorsal or central contralateral SLu. Additionally, four
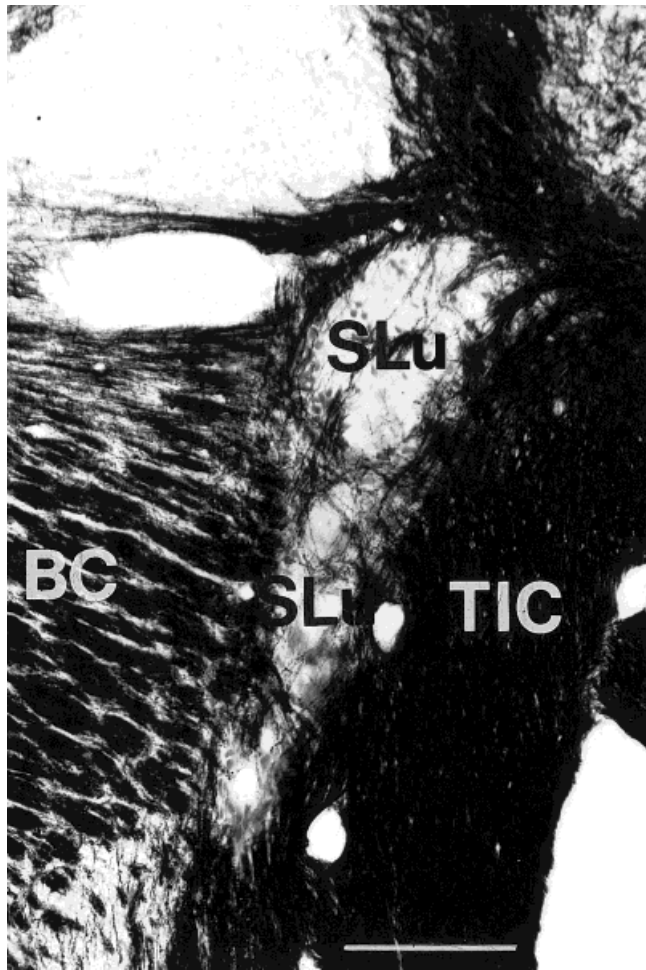
Fig. 2. Gallyas silver impregnation of myelin sheets in the surrounding of SLu. Although only few myelinated fibers cross the SLu, medially oriented fibers seem to invade the brachium conjunctivum (BC) and laterally oriented axons seem to join the tractus isthmocerebellaris (TIC). Scale bar = 500 μm.

rotundal CtB injections revealed retrogradely labeled cells directly rostrally adjacent to the contralateral SLu.

Tectal CtB injections also filled some somata within the contralateral SLu. They were located within its rostralmost tip (overall 2–7 cells counted in one-tenth of all sections; Fig. 7).

Immunohistochemical characterization

Both Ipc and SLu displayed strong ChAT immunoreactivity (Fig. 8). SLu cell bodies were intensely labeled, with numerous processes reaching into the center of the nucleus, where they established a dense netting. ChAT-immunoreactive fiber bundles extended from the medial row of SLu somata into the lateral tegmentum. Additionally, more weakly labeled fiber bundles arose dorsomedially from the SLu. Compared to that in Ipc, the intensity of the somatic labeling was remarkably stronger within SLu. Counting of immunopositive cells and adjacent cresyl violet-stained sections in two animals revealed 91% (SD 6.0) of SLu somata as immunoreactive with the ChAT antibody. ChAT/cresyl violet double labeling revealed

nearly all somata to be immunoreactive, with the exception of the caudalmost SLu, where several neurons remained immunonegative. Nucleus rotundus also exhibited ChAT immunoreactivity, which was confined to thin fiber processes and enhanced diffuse background staining in transverse sections (Fig. 9).

Whereas the Imc was characterized by a cellular GABA immunoreactivity, Ipc and SLu displayed a diffuse neuropil GABA staining in combination with interspersed short fiber segments (Fig. 10). Compared to SLu, Ipc overall labeling intensity was slightly stronger.

SLu neurons exhibited strong somatic immunoreactivity against glutamate receptor subtype GluR1 (Fig. 11), whereas antibodies directed against GluR2/3 subunits revealed no labeled cells except very weak diffuse background staining (Fig. 12). Comparison of cell counts of GluR1-immunoreactive somata and adjacent cresyl violet-stained sections suggested that 90% of SLu cells expressed the AMPA receptor subunit. In contrast, Ipc revealed no immunoreactivity against the GluR1 subunit, although virtually all of its somata were immunopositive for an antibody against the GluR2/3 subunit (Fig. 12).

DISCUSSION

This study reveals that SLu has unique connectivity patterns and immunhistochemical characteristics and is thus a key component of the isthmic complex. As is discussed below, the projections of the SLu onto the tectum, the rotundus, and the SpL (Reiner et al., 1982a) demonstrate that this isthmic structure is possibly able to modulate ascending tectofugal as well as descending visuomotor processes.

Architecture of the semilunar connectivity pattern

Like the other isthmic nuclei (Hunt et al., 1977), SLu exhibits reciprocal connections with the optic tectum. Although the topographic order within the tecto-Imc system is only poor, it is very precise for the tecto-Ipc connection (Hunt and Künzle, 1976; Güntürkün and Remy, 1990). The present data show a comparably tight topographic arrangement for the tecto-SLu projections, with the rostrodorsal and caudoventral tectum being connected to the rostrodorsal and caudoventral SLu, respectively. Data on the tectal targets of the semilunar projection are partly contradictory, in that previous anterograde tracing experiments pointed to a projection onto the intermediate and deep layers (Hunt and Brecha, 1984), whereas our data on the laminar distribution of tectal tracer spread and resulting semilunar labeling suggest a more superficial tectal projection, comparable to that of the Ipc (Hunt and Brecha, 1984; Woodson et al., 1991). Insofar as earlier studies used radioactive tracers with a much larger tracer spread, it is likely that these tracers also labeled other midbrain nuclei surrounding SLu.

In contrast to Ipc data, our data clearly show that SLu ascends onto the diencephalic nucleus rotundus. These newly described rotundally projecting SLu neurons constitute a subgroup of the tectally projecting neurons: Combined tectal and rotundal tracer injections revealed that nearly 50% of rotundally projecting neurons exhibit axon collaterals onto the tectum. In that the semilunar-tectal projection is tightly topographically organized and tracer
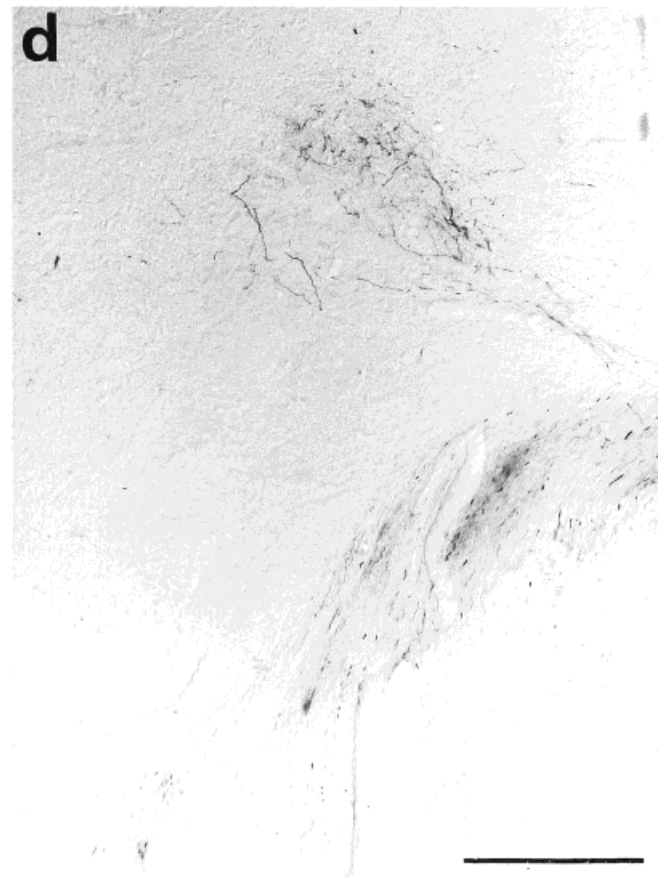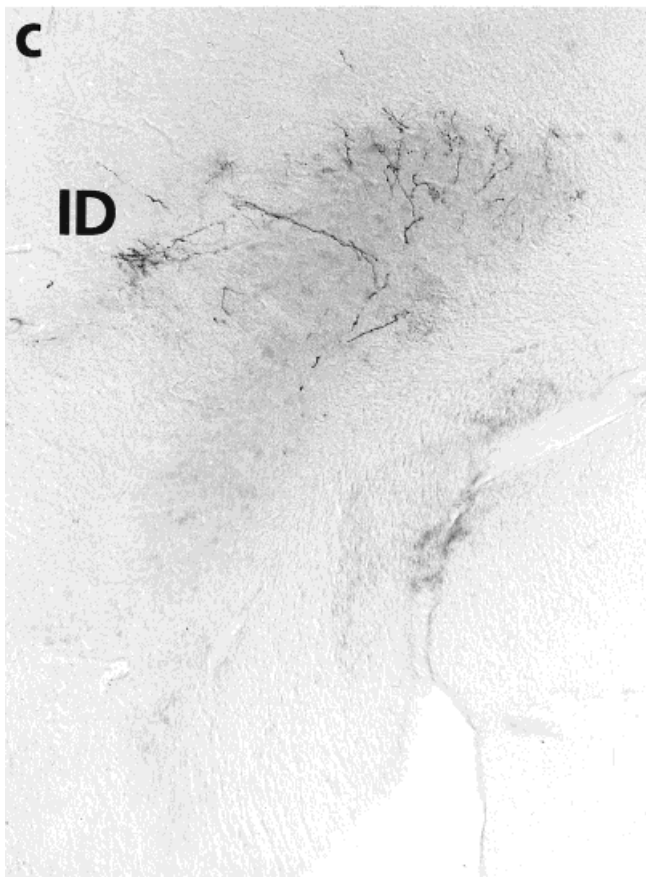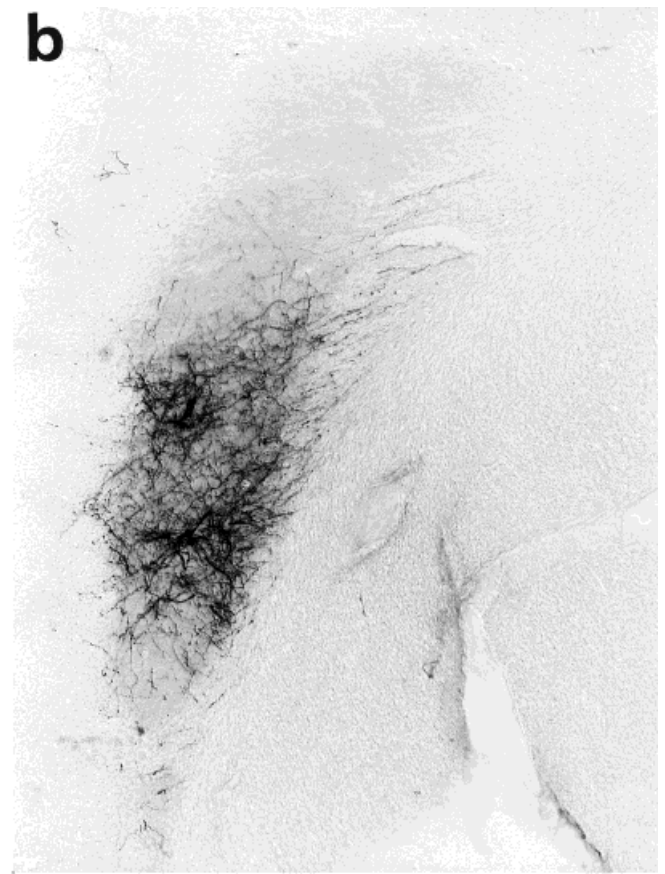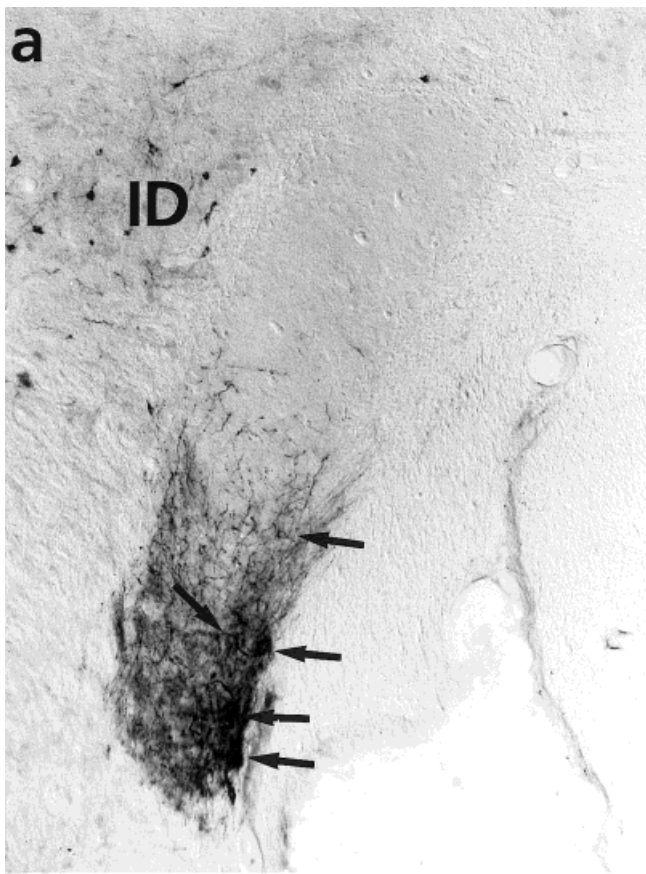
Fig. 3. Anterograde fiber labeling within subcomponents of the SLu after focal CtB or BDA injections into the ipsilateral tectum. **a:** CtB injections into the ventral tectum resulted in anterogradely labeled fibers concentrated within the ventralmost portion of the SLu. Additionally, retrogradely labeled somata (arrows) were located within its ventrolateral tip (masked by fiber fillings) and ID. **b:** An-terogradely labeled fibers within the ventral and central SLu after a BDA injection into the ventrolateral tectum. **c:** BDA labeled fibers within the central and dorsal SLu after an injection into the dorso-lateral tectum. Some additional fiber labeling is visible within the ID. **d:** Anterogradely BDA-labeled fibers within the dorsalmost SLu after a tracer injection restricted to the dorsal tectum. Scale bar = 200 µm.
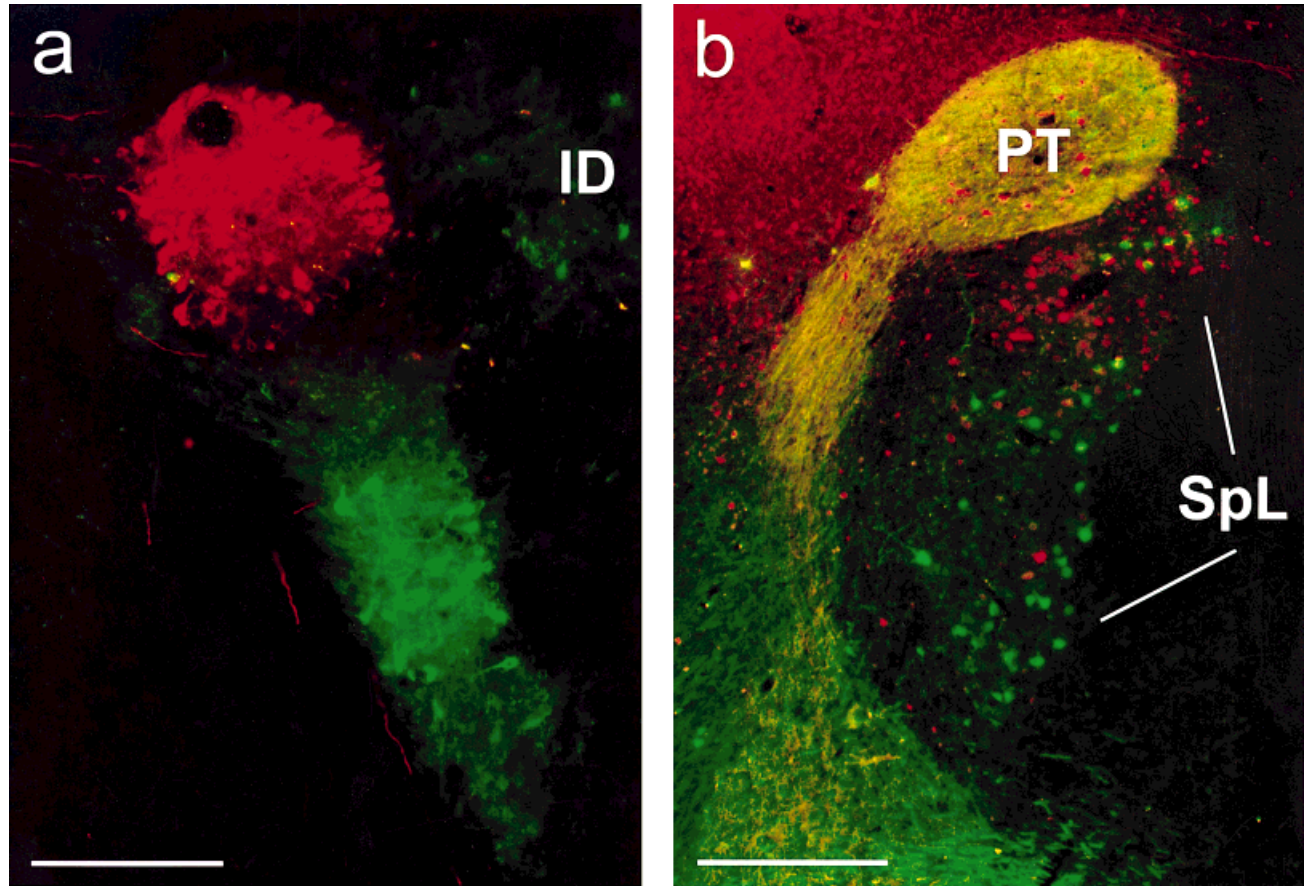
Fig. 4. Retrogradely labeled cells within the SLu (a) and nucleus spiriformis lateralis (SpL; b) after injections of fluorescent dextrans into the ventrolateral (FDA, green) and dorsal tectum (TDA, red). **a:** Cells within the SLu were completely segregated with the dorsal SLu projecting onto the dorsal tectum and the central and ventral SLu projecting onto the ventrolateral tectum. Double-labeled cells (yellow) were restricted to the disseminated isthmic nucleus (ID). **b:** SpL output onto the tectum exhibits a rough topography; projections onto the dorsal tectum (red) were concentrated within the dorsal SpL, whereas cells projecting to the ventrolateral tectum (green) were often located within the ventral and central SpL. PT, nucleus pretectalis. Scale bars = 200 μm in A, 500 μm in B.

spread never covered the entire tectal surface, it is likely that the proportion of rotundally projecting SLu neurons with axon collaterals to the tectum is considerably higher than this.

Focal rotundal CtB injections revealed a roughly topographic order within the SLu-rotundal projection. Thus, within the tectofugal pathway, SLu is interposed as a structure with topographically organized projections onto targets that establish different functional organizations: Whereas the tectum represents a two-dimensional (2D) visual map, the rotundus is characterized by nonretinotopically organized functional domains (Revzin, 1979; Wang et al., 1993). SLu might therefore constitute a critical component in the transition from retinotopic tectal to functionotopic rotundal coding along the tectofugal pathway. To outline this, we will first consider the organization of the tectorotundal projection.

Specific relay cells in lamina 13 of the tectum constitute a massive bilateral projection onto the nucleus rotundus (Benowitz and Karten, 1976). The rotundus itself is compartmentalized in different functional domains, being selective for 2D or 3D movement, color, and luminance (Wang et al., 1993). The transition from retinotopic coding

at the tectal level to functionotopic coding within the rotundus is built up by the regionally discrete projection of at least five morphologically distinct populations of tectal layer 13 neurons (Hellmann and Güntürkün, 2001). Each of these five cell groups has a distinct dendritic ramification pattern within the retinorecipient tectal layers and thus receives an idiosyncratic mixture of retinal ganglion cell input. It is therefore very likely that these neurons have distinct visual response properties. Because these cells terminate in five different rotundal domains, this visual specificity is transposed onto nucleus rotundus. Thus, the tectorotundal projection is characterized by the presence of at least five parallel streams of heterogeneous visual coding. However, there is a further variable that characterizes the tectorotundal projection: Tectal lamina 13 cells also differ quantitatively with respect to their overall distribution over the tectal surface. Although two cell populations predominantly, but not exclusively, cluster in the ventral tectum, one is primarily located within the dorsal tectum (Hellmann and Güntürkün, 2001). The tectum is retinotopically organized, with the upper visual field represented in the dorsal and the lower visual field in the ventral tectum, so these cell-type specific distributions
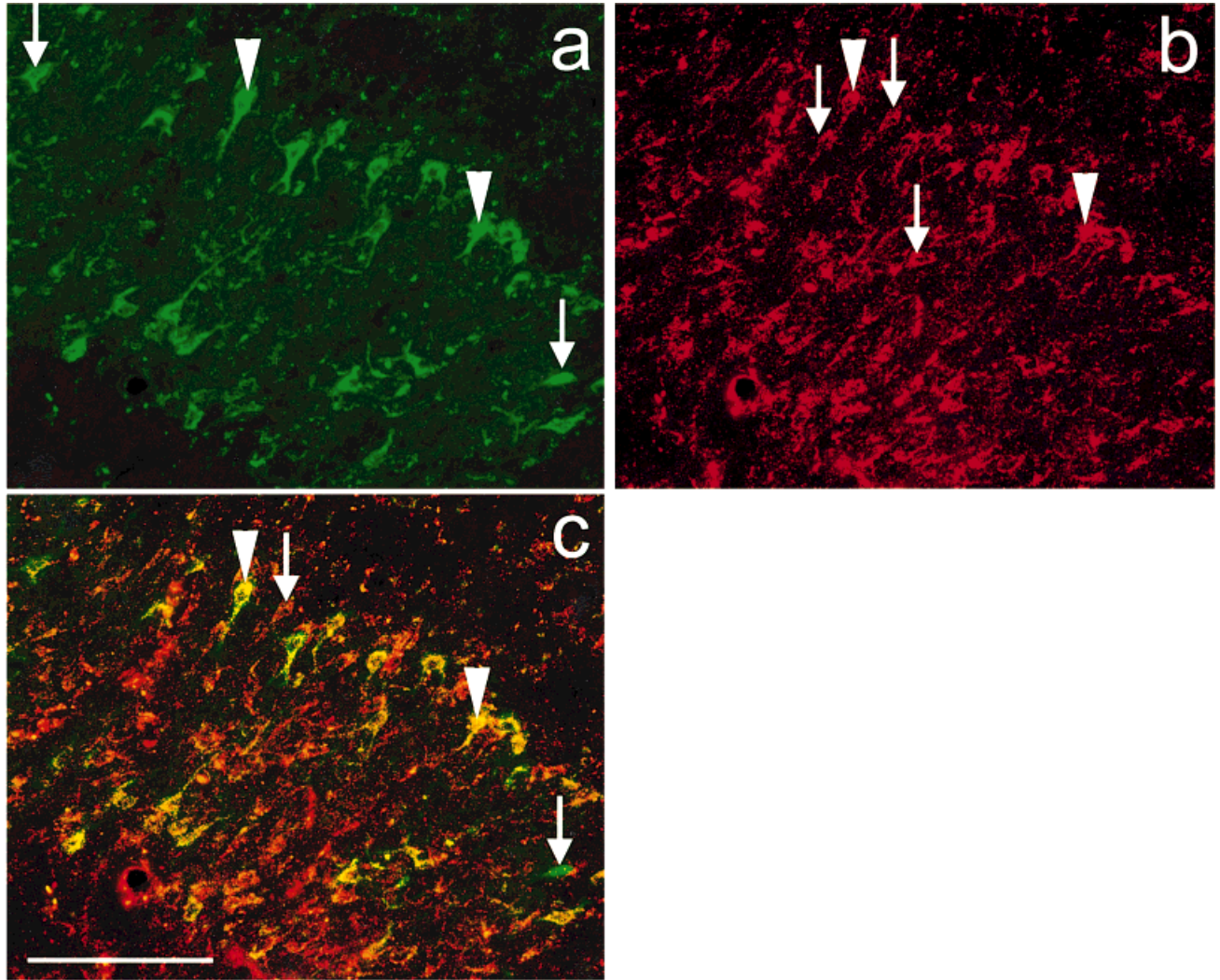
Fig. 5. **a–c:** Retrogradely labeled cells within the SLu after rotundal CtB injections (green fluorescence in a,c) and multiple TDA injections into the ipsilateral tectum (red in b,c). Within the corresponding frames, arrowheads in a–c point to double-labeled cells (yellow in the compound figure, c). Arrows point to cells labeled with only one tracer. Scale bar = 100 μm.

should result in a visual field-related specificity of the tectorotundal transition (Hellmann and Güntürkün, 1999). Taken together, the parallel tectorotundal streams can be compartmentalized according to their differential visual coding principles as well as according to their visual field specificity.

Apart from the direct tectorotundal pathway, indirect projections also connect tectum and rotundus. One of them is the tectopretectorotundal system, which connects to nucleus rotundus via three pretectal nuclei, each receiving input via collaterals of the tectorotundal projection (Deng and Rogers, 1998). Insofar as each rotundal domain also receives a domain-specific mixture of afferents from the three pretectal nuclei, the pretectorotundal connectivity mirrors the whole compartmentalization of the tectorotundal system (Deng and Rogers, 1998; Hellmann and Güntürkün, 2001). The second indirect tectorotundal sideway, the tectosemilunar-rotundal system, is described for

the first time in the present paper. This pathway seems to be especially organized according to a visual field-specific differentiation: Dorsal SLu is reciprocally connected to dorsal tectum and projects to caudal rotundus. Because caudal rotundus receives mainly afferents from dorsal tectum (Hellmann and Güntürkün,2001) and because the dorsal tectum receives input from the upper visual field (Remy and Güntürkün, 1991), the dorsal tectum-dorsal Slu-caudal rotundus system seems to be a tightly interlinked pathway to process stimuli from the superior visual field. The ventral tectum is interconnected to ventral SLu, with both structures projecting to the remaining rotundal domains (Fig. 13). At least some of these domains receive mainly ventral tectal afferents (Hellmann and Güntürkün, 2001). Therefore, the ventral tectum-ventral Slu-rostral rotundus system processes mainly, but not exclusively, input from the lower visual field. Taken together, the functional organization within the tectosemilunar-
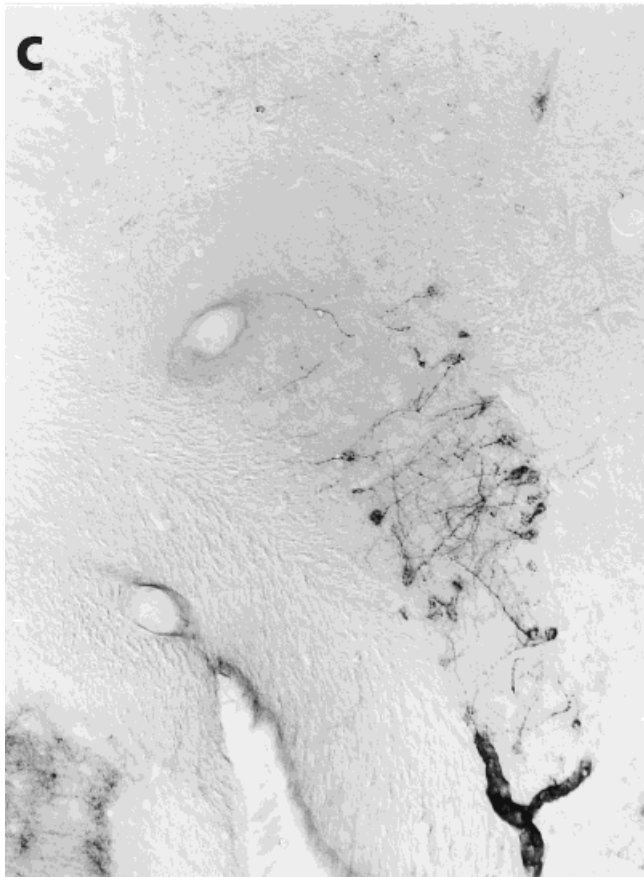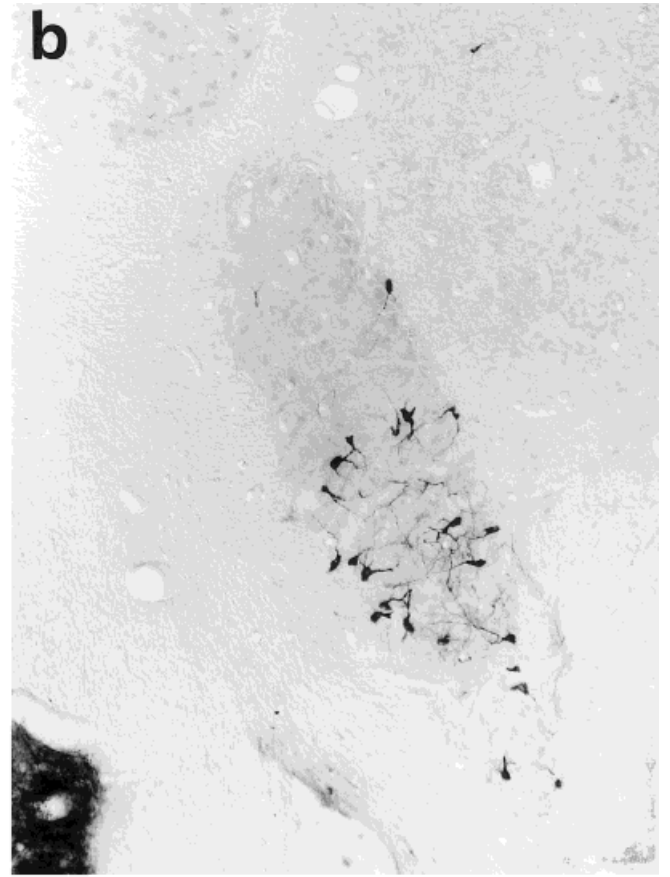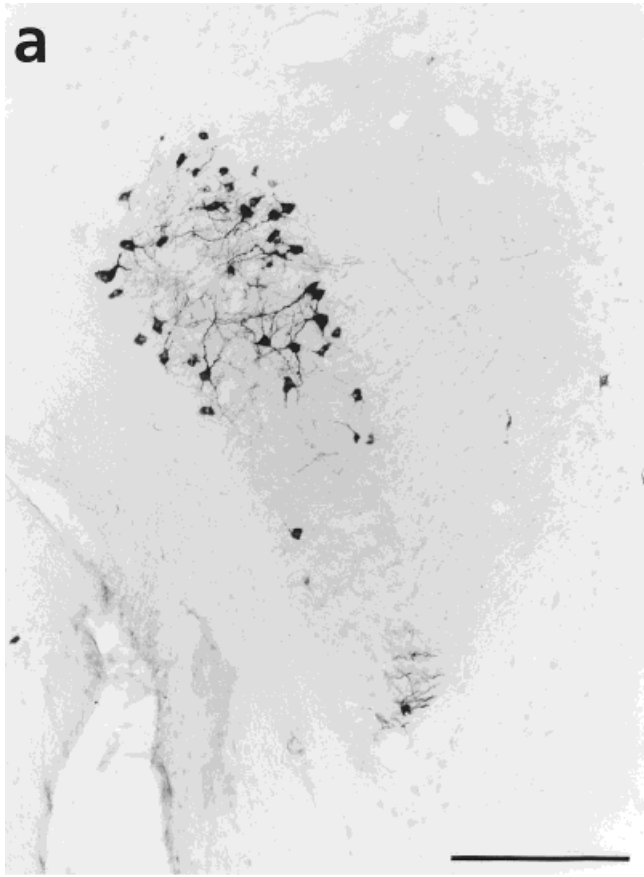
Fig. 6. Semilunar labeling patterns after CtB injections into distinct portions of the nucleus rotundus that are characterized by a differential input from tectal cell populations (Hellmann and Güntürkün, 2001). **a:** CtB injections into the caudalmost rotundus labeled somata predominately within the dorsal SLu. **b:** CtB injections into the ventral rotundus labeled cells within the central and ventral SLu. **c:** The same semilunar labeling pattern resulted after CtB injections into the rostrodorsal rotundus. Scale bar = 200 μm.

Fig. 7. Somata labeled within the rostral one-third of the SLu after CtB injection into contralateral tectum. Scale bar = 500 μm.

Fig. 8. ChAT-like immunoreactivity within SLu and Ipc. SLu somata were intensely labeled. In addition, numerous processes exhibit strong immunoreactivity. Comparatively weaker ChAT staining was obvious in the dorsally adjoining Ipc. Scale bar = 500 μm.

rotundal system seems to be governed mainly by a differential modulation of visual field-specific information.

In addition to the projection onto two components of the tectofugal system, SLu exerts output to the lateral spiriform nucleus (SpL), which conveys basal ganglia influence onto the tectum and hence participates in controlling the tectal premotor output (Jiao et al., 2000; Reiner et al., 1982a). Thus, SLu modulates tectal information processing not only directly via its projections onto the presumably outer retinorecipient layers but also indirectly via the SpL, which innervates the deeper tectal layers, from which the descending projections arise (Reiner and Karten, 1982; Reiner et al., 1982a).

As do the ascending tectorotundal and SLu-rotundal connections, the SpL-tectal projection exhibits a visual field specificity along the dorsoventral tectal axis (Reiner et al., 1982a; Fig. 4b). Therefore, it is likely that visual field-dependent specifications are not restricted to the ascending information stream but are also present along the entire tecto-SLu-SpL-tectum loop and hence might constitute a characteristic feature of visuomotor integration.

Immunohistochemical characteristics of the SLu

Like Ipc, SLu is labeled by a dense network of GABA-immunoreactive fibers (Fig. 9). In addition, neurons of both nuclei exhibit immunoreactivity against AMPA-receptor subunits constituting ionotropic glutamate receptors in a pentameric arrangement (Fagg, 1985). The functional characteristics of the AMPA receptors are determined by the specific combination of the receptor subunits, whereby GluR2 controls their calcium permeability (Boulter et al., 1990; Keinänen et al., 1990), so, in addition to their comparable reciprocal connections with the tectum, both nuclei share GABAergic as well as glutamatergic input. However, the action of at least glutamate may vary between Ipc and Slu, because they express different AMPA-receptor subunits, with Ipc exclusively expressing GluR1 and SLu expressing GluR2/3.

Nearly all somata of Ipc and SLu were shown to exhibit somatic immunoreactivity against ChAT (Medina and Reiner, 1994; Sorenson et al., 1989), a specific marker for cholinergic neurons. The present study confirms these data and also reveals a much stronger somatic ChAT immunreactivity in SLu compared to Ipc. In that more than 90% of somata are ChAT-positive, one would expect acetylcholine (ACh) to be the transmitter of the semilunar-rotundal projection. Available data on a cholin-
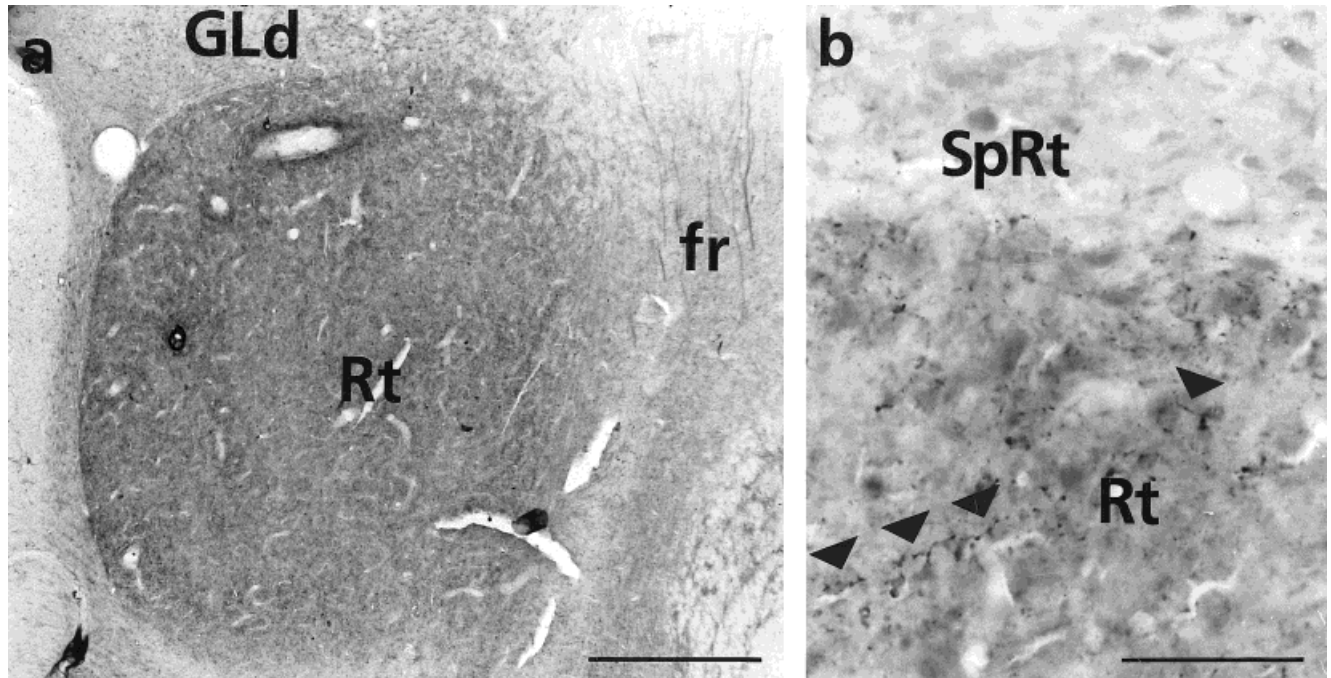
Fig. 9. ChAT-like immunoreactivity within the thalamus. **a:** Compared to the dorsolateral thalamus (GLd), nucleus rotundus (Rt) exhibits enhanced binding with the ChAT antibody. ChAT-immunoreactive fibers were also labeled in the fasciculus retroflexus (fr). **b:** Higher magnification of nucleus Rt and the dorsally adjoining nucleus suprarotundus (SpRt), which is a part of the GLd. Arrowheads point to ChAT-immunoreactive fiber processes. Scale bars = 500 μm in A, 50 μm in B.
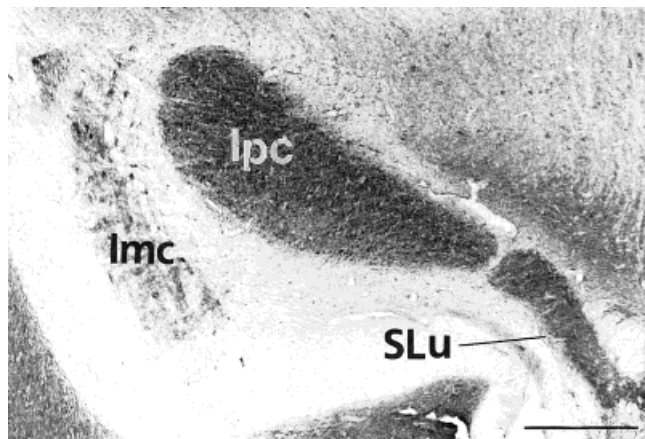
Fig. 10. Overview of GABA-like immunoreactivity within the isthmic nuclei. Whereas Imc exhibited somatic labeling, Ipc and SLu were characterized by intense diffuse labeling. Scale bar = 500 μm.

ergic innervation of the rotundus are contradictory. The rotundus exhibits moderate to high levels of acetylcholinesterase activity, a marker for cholinergic as well as cholinoceptive neurons (Martinez-de-la-Torre et al., 1990; Vischer et al., 1982). Receptor binding studies revealed high affinity of muscarinic Ach receptor ligands within the dorsal rotundus/nucleus triangularis (Dietl et al., 1988), but this could also indicate a cholinergic projection from the medial habenula to nucleus triangularis (Sorenson et al., 1989). The remaining rotundus is characterized by low

(Vischer et al., 1982; Watson et al., 1988) to moderate (Britto et al., 1992; Sorenson and Chiappinelli, 1992) levels of nicotinic receptors. ChAT-immunoreactive fibers were found within the rotundus of chicks (Sorenson et al., 1989). The present study confirms these results also in pigeons, although a previous study in the same species failed to show intrarotundal ChAT immunoreactivity (Medina and Reiner, 1994). A possible explanation for the different results is that rotundal labeling was confined to thin fiber processes, without strongly enhanced diffuse tissue staining.

Although Ach can principally exert excitatory as well as inhibitory actions, Wang et al. (1995) demonstrated an excitatory action of ACh at least for the Ipc recipient pool of tectal units. The immunohistochemical characterization of the three rotundally projecting systems suggests the existence of differential physiological actions on rotundal neurons. Whereas the direct glutamatergic tectorotundal projection exerts excitatory influences onto the rotundus (Huang et al., 1998), the indirect pathways might modulate rotundal processing in an opposing way, with inhibitory (GABAergic) input from the pretectum (Gao et al., 1995; Mpodozis et al., 1996) and a cholinergic innervation from the SLu for which presently no physiological information exists.

Isthmothalamic projections in other vertebrates

Nucleus isthmi, defined as a midbrain region with reciprocal and topographically organized connections with the tectum opticum, is present in most if not all vertebrates (see introductory paragraphs). Studies in reptiles
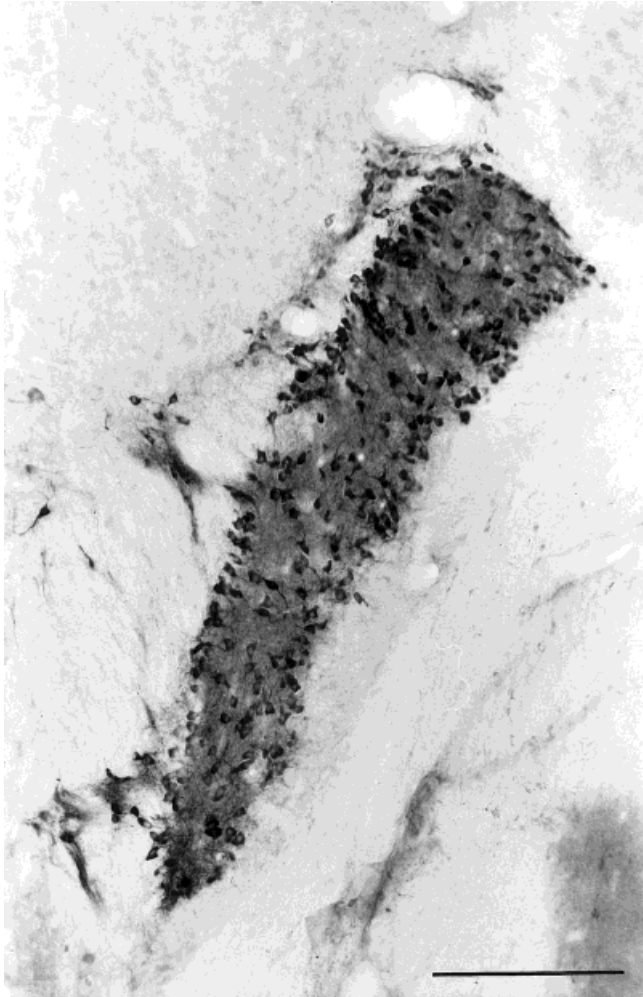
Fig. 11. Immunoreactivity against the AMPA receptor subunit GluR1 within the SLu. In addition to diffuse background staining throughout the SLu, most of its cells were intensely labeled. Scale bar = 200 µm.

Fig. 12. Overview of the differential immunoreactivity for glutamate receptor subunits within the isthmic nuclei. **a:** GluR1 immunoreactivity was nearly confined to the SLu. **b:** Many GluR2/3-positive somata were labeled within Imc and Ipc, whereas SLu exhibited weak background labeling. Scale bar = 500 µm.

and mammals demonstrated, in addition to its tectal connections, a projection onto the rotundus (Berson and Hartline, 1988), and its mammalian equivalent, the colliculus-recipient posterolateral pulvinar (cat: Spreafico et al., 1980; monkeys: Benevento and Standage, 1983; Diamond et al., 1992). The existence of an isthmorotundal projection within all amniotes suggests isthmothalamic projections to constitute an ancient feature of the isthmic connectivity pattern. However, within the scope of the phylogenetic subdifferentiation of the avian isthmic complex, only one substructure, the SLu, establishes an ascending projection presumably in response to its specific role within the isthmic complex.

The parabigeminal nucleus, the mammalian homologue of the nucleus isthmi, also projects onto the thalamic center of the geniculocortical visual pathway (Benevento and Standage, 1983; Graybiel, 1978; Hashikawa et al., 1986). Its avian counterpart, the nucleus geniculatus lateralis, pars dorsalis (GLd), was shown to exhibit strong ChAT activity (Vischer et al., 1982) as well as immunore-

activity against ChAT (Güntürkün and Karten, 1991). In addition, immuncytochemical data (Britto et al., 1992; Lohmann et al., 2000; Sorenson et al., 1989) and ligand-binding studies (Sorenson and Chiappinelli, 1992; Watson et al., 1988) confirmed high levels of nicotinic ACh receptors within GLd. Thus, a cholinergic projection of SLu onto GLd could in principle be possible in pigeons, but our control experiments, which included CtB injections within wide regions of the dorsal thalamus, including GLd, could rule out this possibility.

Taken together, the SLu assumes a highly specific position within the concert of the isthmic nuclei. Unlike the Ipc and Imc, it is not only reciprocally connected to the tectum but also projects onto the rotundus and the SpL. Its role thus goes far beyond a local modulation of intratectal processes.

ACKNOWLEDGMENTS
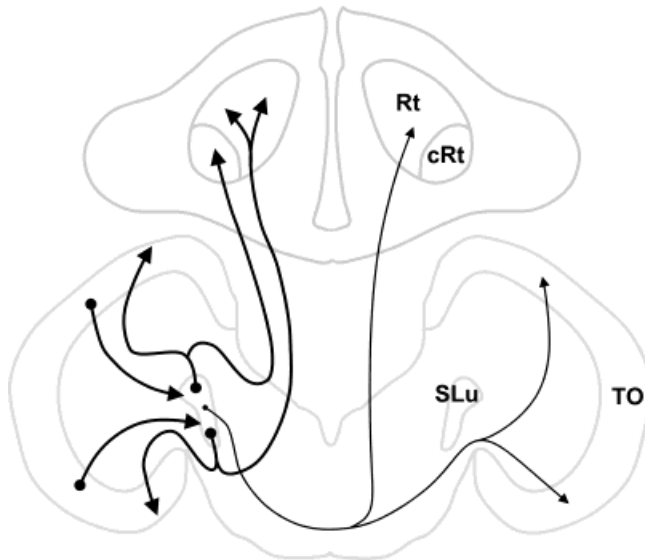
Fig. 13. Schematic summary of the connectivity pattern of nucleus semilunaris. SLu exhibits tight topographic and reciprocal connections with the ipsilateral tectum. Axon collaterals of tectally projecting neurons also innervate nucleus rotundus in a roughly topographic manner. This resembles the weak topologic order of the direct tecto-rotundal projection, which is characterized by predominantly dorsal tectal input to the caudal rotundus and a dominance of ventral tectal input to the ventral and central rotundal domains (Hellmann and Güntürkün, 1999, 2001). cRt, caudal rotundal domain; Rt, remaining rotundal domains; SLu, nucleus semilunaris; TO, tectum opticum.

LITERATURE CITED

Acheson DW, Kemplay SK, Webster KE. 1980. Quantitative analysis of optic terminal profile distribution within the pigeon optic tectum. Neuroscience 5:1067–1084.

Adams JC. 1981. Heavy metal intenisification of DAB-based HRP reaction product. J Histochem Cytochem 29:775.

Bagnoli P, Francesconi W, Magni F. 1979. Interaction of optic tract and visual wulst impulses on single units of the pigeon's optic tectum. Brain Behav Evol 16:19–37.

Bagnoli P, Fontanesi G, Alesci R, Erichsen JT. 1992. Distribution of neuropeptide Y, substance P, and choline acetyltransferase in the developing visual system of the pigeon and effects of unilateral retina removal. J Comp Neurol 318:392–414.

Baleydier C, Magnin M. 1979. Afferent and efferent connections of the parabigeminal nucleus in cat revealed by retrograde axonal transport of horseradish peroxidase. Brain Res 161:187–198.

Benevento LA, Standage GP. 1983. The organization of projections of the retinorecipient and nonretinorecipient nuclei of the pretectal complex and layers of the superior colliculus to the lateral pulvinar and medial pulvinar in the macaque monkey. J Comp Neurol 217:307–336.

Benowitz LI, Karten HJ. 1976. Organization of tectofugal visual pathway in pigeon: retrograde transport study. J Comp Neurol 167:503–520.

Berson DM, Hartline PH. 1988. A tecto-rotundo-telencephalic pathway in the rattlesnake: evidence for a forebrain representation of the infrared sense. J Neurosci 8:1074–1088.

Boulter J, Hollmann M, O'Shea-Greenfield A. 1990. Molecular cloning and functional expression of glutamate receptor subunit genes. Science 249:1033–1037.

Britto LR, Keyser KT, Lindstrom JM, Karten HJ. 1992. Immunohistochemical localization of nicotinic acetylcholine receptor subunits in the mesencephalon and diencephalon of the chick (Gallus gallus). J Comp Neurol 317:325–340.

Deng C, Rogers LJ. 1998. Organisation of the tectorotundal and SP/IPS-rotundal projections in the chick. J Comp Neurol 394:171–185.

Diamond IT, Fitzpatrick D, Conley M. 1992. A projection from the parabigeminal nucleus to the pulvinar nucleus in Galago. J Comp Neurol 316:375–382.

Dietl MM, Cortes R, Palacios JM. 1988. Neurotransmitter receptors in the avian brain. II. Muscarinic cholinergic receptors. Brain Res 439:360–365.

Domenici L, Waldvogel HJ, Matute C, Streit P. 1988. Distribution of GABA-like immunoreactivity in the pigeon brain. Neuroscience 25:931–950.

Duff TA, Scott G, Mai R. 1981. Regional differences in pigeon optic tract, chiasm, and retino-receptive layers of optic tectum. J Comp Neurol 198:231–247.

Fagg GE. 1985. L-glutamate, excitatory amino acid receptors and brain function. Trends Neurosci 8:207–210.

Gao HF, Wu GY, Frost BJ, Wang SR. 1995. Excitatory and inhibitory neurotransmitters in the nucleus rotundus of pigeons. Vis Neurosci 12:819–825.

Granda AM, Crossland WJ. 1989. GABA-like immunoreactivity of neurons in the chicken diencephalon and mesencephalon. J Comp Neurol 287:455–469.

Graybiel AM. 1978. A satellite system of the superior colliculus: the parabigeminal nucleus and its projections to the superficial collicular layers. Brain Res 28:365–374.

Gruberg ER, Udin SB. 1978. Topographic projections between the nucleus isthmi and the tectum of the frog Rana pipiens. J Comp Neurol 179:487–500.

Güntürkün O. 1987. A Golgi study of the isthmic nuclei in the pigeon (Columba livia). Cell Tissue Res 248:439–448.

Güntürkün O. 2000. Sensory physiology: vision. In: Whittow GC, editor. Sturkie's avian physiology, 5th ed. San Diego: Academic Press. p 1–19.

Güntürkün O, Hahmann U. 1999. Functional subdivisions of the ascending visual pathways in the pigeon. Behav Brain Res 98:193–201.

Güntürkün O, Karten HJ. 1991. An immunocytochemical analysis of the lateral geniculate complex in the pigeon (Columba livia). J Comp Neurol 314:721–749.

Güntürkün O, Remy M. 1990. The topographical projection of the nucleus isthmi pars parvocellularis (Ipc) onto the tectum opticum in the pigeon. Neurosci Lett 111:18–22.

Hashikawa T, Van Lieshout D, Harting JK. 1986. Projections from the parabigeminal nucleus to the dorsal lateral geniculate nucleus in the tree shrew Tupaia glis. J Comp Neurol 246:382–394.

Hayes BP, Webster KE. 1985. Cytoarchitectural fields and retinal termination: an axonal transport study of laminar organization in the avian optic tectum. Neuroscience 16:641–657.

Hellmann B, Güntürkün O. 1999. Visual-field-specific heterogeneity within the tecto-rotundal projection of the pigeon. Eur J Neurosci 11:2635–2650.

Hellmann B, Güntürkün O. 2001. Structural organization of parallel information processing within the tectofugal visual system of the pigeon. J Comp Neurol 429:94–112.

Huang LH, Li JL, Wang SR. 1998. Glutamatergic neurotransmission from the optic tectum to the contralateral nucleus rotundus in pigeons. Brain Behav Evol 52:55–60.

Hunt SP, Brecha N. 1984. The avian optic tectum: a synthesis of morphology and biochemistry. In: Vanegas H, editor. Comparative neurology of the optic tectum. New York: Plenum Press. p 619–648.

Hunt SP, Künzle H. 1976. Observations on the projections and intrinsic organization of the pigeon optic tectum: an autoradiographic study based on anterograde and retrograde, axonal and dendritic flow. J Comp Neurol 170:153–172.

Hunt SP, Streit P, Kunzle H, Cuenod M. 1977. Characterization of the pigeon isthmo-tectal pathway by selective uptake and retrograde movement of radioactive compounds and by Golgi-like horseradish peroxidase labeling. Brain Res 129:197–212.

Ito H, Sakamoto N, Takatshji K. 1982. Cytoarchitecture, fiber connections, and ultrastructure of nucleus isthmi in a teleost (Navodon modestus) with a special reference to degenerating isthmic afferents from optic tectum and nucleus pretectalis. J Comp Neurol 205:299–311.

Jiao Y, Medina L, Veenman CL, Toledo C, Puelles L, Reiner A. 2000. Identification of the anterior nucleus of the ansa lenticularis in birds as the homolog of the mammalian subthalamic nucleus. J Neurosci 20:6998–7010.

Karten HJ, Hodos W. 1967. A stereotaxic atlas of the brain of the pigeon. Baltimore: Johns Hopkins Press.

Karten HJ, Cox K, Mpodozis J. 1997. Two distinct populations of tectal neurons have unique connections within the retinotectorotundal pathway of the pigeon (Columba livia). J Comp Neurol 387:449–465.

Keinänen K, Wisden W, Sommer B. 1990. A family of AMPA-selective glutamate receptors. Science 249:556–560.

Künzle H, Schnyder H. 1984. The isthmus–tegmentum complex in the turtle and rat: a comparative analysis of its interconnections with the optic tectum. Exp Brain Res 56:509–522.

Lohmann TH, Torrao AS, Britto LR, Lindstrom J, Hamassaki-Britto DE. 2000. A comparative nonradioactive in situ hybridization and immunohistochemical study of the distribution of alpha7 and alpha8 subunits of the nicotinic acetylcholine receptors in visual areas of the chick brain. Brain Res 852:463–469.

Martinez-De-La-Torre M, Martinez S, Puelles L. 1990. Acetylcholinesterase-histochemical differential staining of subdivisions within the nucleus rotundus in the chick. Anat Embryol 181:129–135.

Medina L, Reiner A. 1994. Distribution of choline acetyltransferase immunoreactivity in the pigeon brain. J Comp Neurol 342:497–537.

Mpodozis J, Cox K, Shimizu T, Bischof HJ, Woodson W, Karten HJ. 1996. GABAergic inputs to the nucleus rotundus (pulvinar inferior) of the pigeon (*Columba livia*). J Comp Neurol 374:204–222.

Northcutt RG. 1982. Localization of neurons afferent to the optic tectum in longnose gars. J Comp Neurol 204:325–335.

Reiner A, Karten HJ. 1982. Laminar distribution of the cells of origin of the descending tectofugal pathways in the pigeon (*Columba livia*). J Comp Neurol 204:165–187.

Reiner A, Brecha NC, Karten HJ. 1982a. Basal ganglia pathways to the tectum: the afferent and efferent connections of the lateral spiriform nucleus of pigeon. J Comp Neurol 208:16–36.

Reiner A, Karten HJ, Brecha NC. 1982b. Enkephalin-mediated basal ganglia influences over the optic tectum: immunohistochemistry of the tectum and the lateral spiriform nucleus in pigeon. J Comp Neurol 208:37–53.

Remy M, Güntürkün O. 1991. Retinal afferents to the tectum opticum and the n. opticus principalis thalami in the pigeon. J Comp Neurol 305:57–70.

Revzin AM. 1979. Functional localization in the nucleus rotundus. In: Granda AM, Maxwell HJ, editors. Neural mechanisms of behavior in the pigeon. New York: Plenum Press. p 165–175.

Sakamoto N, Ito H, Ueda S. 1981. Topographic projections between the nucleus isthmi and the optic tectum in a teleost. *Navodon modestus*. Brain Res 224:225–234.

Sereno MI, Ulinski PS. 1987. Caudal topographic nucleus isthmi and the rostral nontopographic nucleus isthmi in the turtle, *Pseudemys scripta*. J Comp Neurol. 261:319–346.

Sherk H. 1979. Connections and visual-field mapping in cat's tectoparabigeminal circuit. J Neurophysiol 42:1656–1668.

Shu SY, Ju G, Fan L. 1988. The glucose oxidase-DAB-nickel method in peroxidase histochemistry of the nervous system. Neurosci Lett 85:169–171.

Sorenson EM, Chiappinelli VA. 1992. Localization of ^{3}H-nicotine, ^{125}I-kappa-bungarotoxin, and ^{125}I-alpha-bungarotoxin binding to nicotinic sites in the chicken forebrain and midbrain. J Comp Neurol 323:1–12.

Sorenson EM, Parkinson D, Dahl JL, Chiappinelli VA. 1989. Immunohistochemical localization of choline acetyltransferase in the chicken mesencephalon. J Comp Neurol 281:641–657.

Spreafico R, Kirk C, Franceschetti S, Avanzini G. 1980. Brain stem projections in the pulvinar-lateralis posterior complex of the cat. Exp Brain Res 40:209–220.

Theiss C, Hellmann B, Güntürkün O. 1998. The differential distribution of AMPA-receptor subunits in the tectofugal system of the pigeon. Brain Res 785:114–128.

Tömböl T, Németh A. 1998. GABA-immunohistological observations, at the electron-microscopic level, of the neurons of isthmic nuclei in chicken, *Gallus domesticus*. Cell Tissue Res 291:255–266.

Veenman CL, Reiner A. 1994. The distribution of GABA-containing perikarya, fibers, and terminals in the forebrain and midbrain of pigeons, with particular reference to the basal ganglia and its projection targets. J Comp Neurol 339:209–250.

Vischer A, Cuenod M, Henke H. 1982. Neurotransmitter receptor ligand binding and enzyme regional distribution in the pigeon visual system. J Neurochem 38:1372–1382.

Wang SR, Yan K, Wang Y, Jiang S, Wang X. 1983. Neuroanatomy and electrophysiology of the lacertian nucleus isthmi. Brain Res 275:355–360.

Wang SR, Wu GY, Felix D. 1995. Avian Imc-tectal projection is mediated by achetylcholine and glutamate. Neuroreport 6:757–760.

Wang YC, Frost BJ. 1991. Visual response characteristics of neurons in the nucleus isthmi magnocellularis and nucleus isthmi parvocellularis of pigeons. Exp Brain Res 87:624–633.

Wang YC, Jiang S, Frost BJ. 1993. Visual processing in pigeon nucleus rotundus: luminance, color, motion, and looming subdivisions. Vis Neurosci 10:21–30.

Wang Y, Xiao J, Wang SR. 2000. Excitatory and inhibitory receptive fields of tectal cells are differentially modified by magnocellular and parvocellular divisions of the pigeon nucleus isthmi. J Comp Physiol 186A:505–511.

Wang YT, Wang SR. 1990. Applications of a carbocyanine fluorescent dye to tracing neuronal connections of the pigeon tectum with some mesencephalic nuclei. Acta Biophys Sin 6:112–116.

Watson JT, Adkins-Regan E, Whiting P, Lindstrom JM, Podleski TR. 1988. Autoradiographic localization of nicotinic acetylcholine receptors in the brain of the zebra finch (*Poephila guttata*). J Comp Neurol 274:255–264.

Welker E, Hoogland PV, Lohmann AHM. 1983. Tectal connections in *Python reticulatus*. J Comp Neurol 220:347–354.

Wiggers W, Roth G. 1991. Anatomy, neurophysiology and functional aspects of the nucleus isthmi in salamanders of the family Plethodontidae. J Comp Physiol 169A:165–176.

Woodson W, Reiner A, Anderson K, Karten HJ. 1991. Distribution, laminar location, and morphology of tectal neurons projecting to the isthmooptic nucleus and the nucleus isthmi, pars parvocellularis in the pigeon (*Columba livia*) and chick (*Gallus domesticus*): a retrograde labelling study. J Comp Neurol 305:470–488.